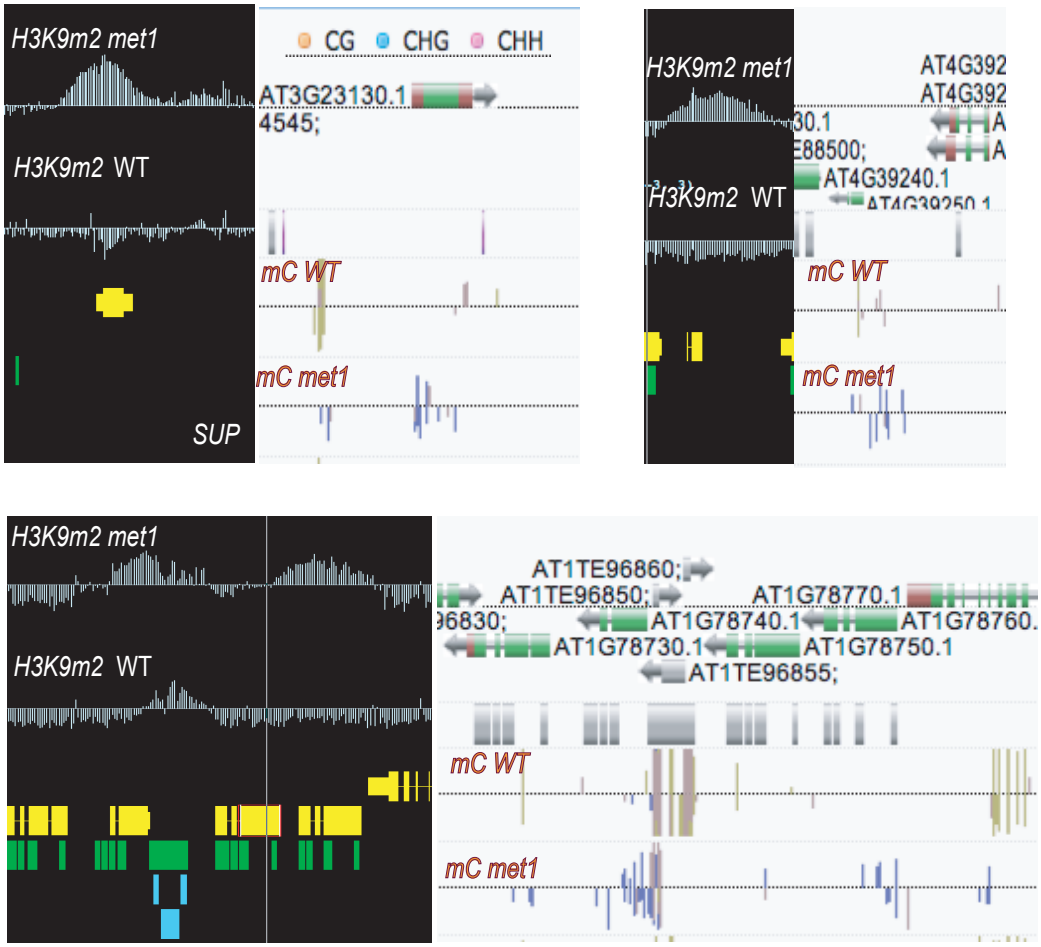

Supplemental Figure 1. Genes showing ectopic H3K9 dimethylation in this study are DNA hypermethylated in *Lister et al.* study. Representative views of genes that gain H3K9m2 marks in their coding-region in *met1* mutants. Representative IGB views (left) and screenshots of the AnnoJ Arabidopsis epigenome browser (http://neomorph.salk.edu/epigenome/epigenome.html) (left) are shown. Yellow horizontal bars: protein-coding genes; blue horizontal bars: transposable elements, green bars: dispersed repeats (i.e. regions of sequence homology); vertical blue bar: relative H3K9m2 levels.

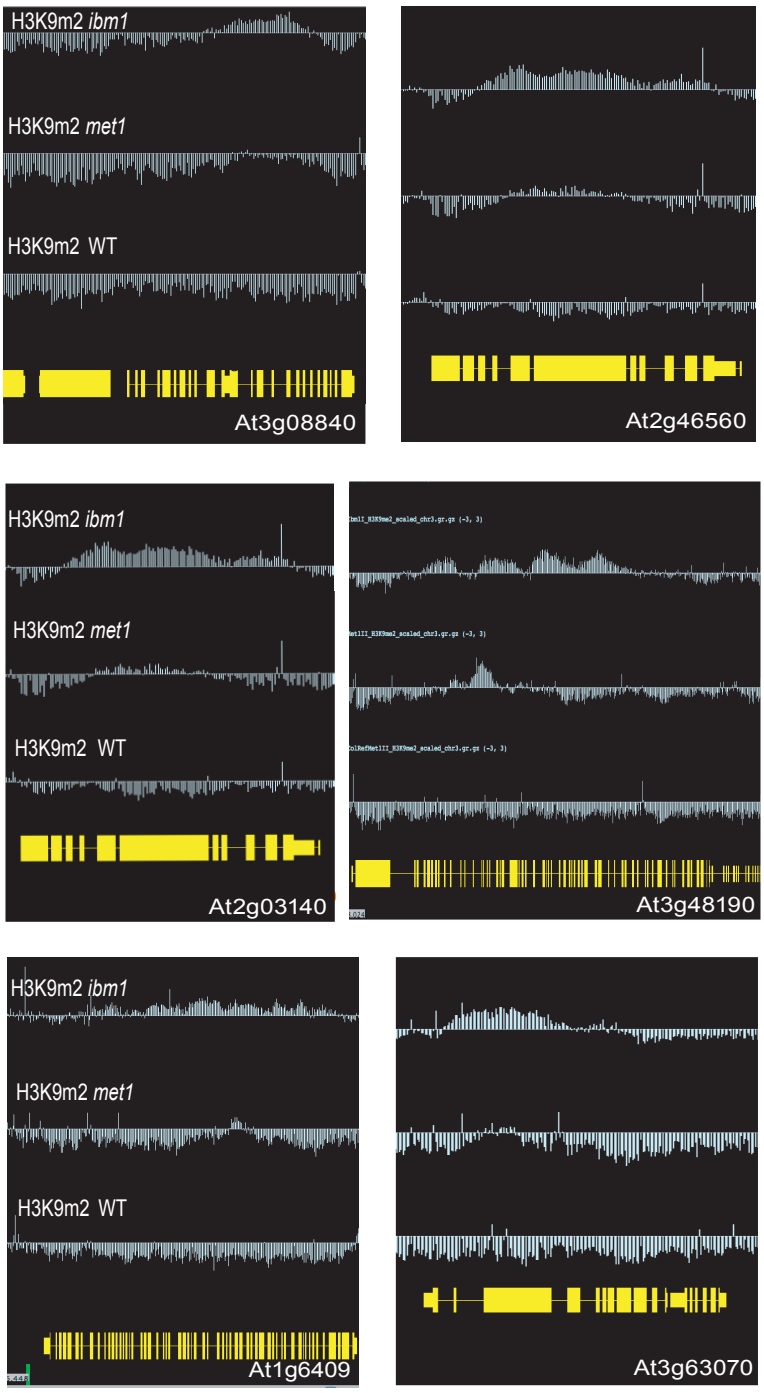

Supplemental Figure 2. Representative views of genes that gain H3K9m2 marks in their body in both *ibm1* and *met1* mutants. We observed that H3K9m2 hypermethylation in *met1* was usually not as extensive as in *ibm1* in accordance with the idea that these genes may be targets of IBM1, the levels of which are reduced in *met1*.Yellow horizontal bars: protein-coding genes; blue horizontal bars: transposable elements; vertical blue bar: relative H3K9m2 levels.

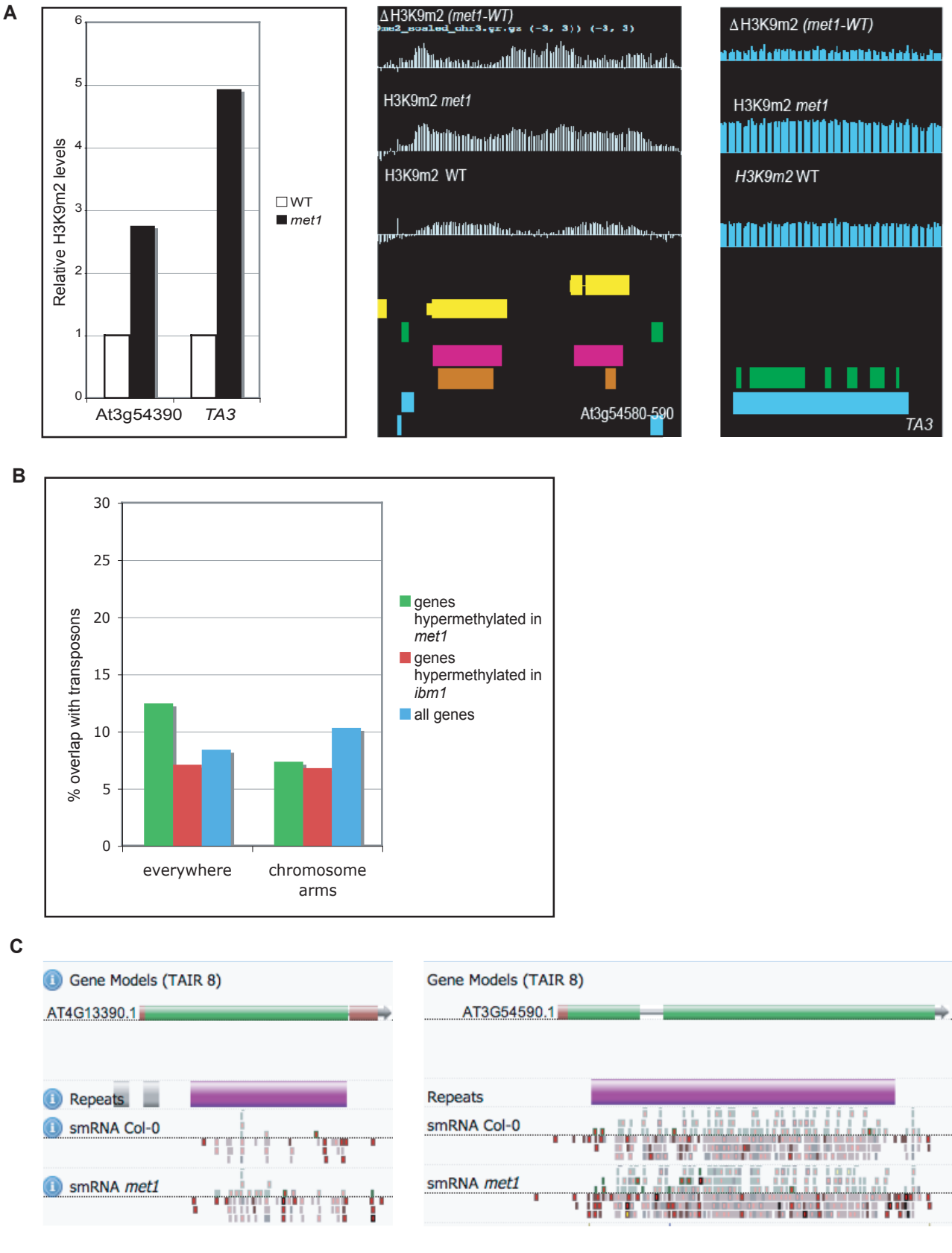

Supplemental Figure 3. Supplementary information on Class I genes. **A.** Verification of H3K9m2 states at genes pre-marked with H3K9m2 in wild type that gain H3K9m2 in *met1* (class I genes) by independent chromatin immunoprecipitation experiments. The immunoprecipitated DNA corresponding to a Class I gene (At3g54590) and a transposable element (*TA3*), -shown to be hypermethylated in the ChIP-chip analysis- was quantified by real-time PCR and normalized to the input DNA and to an internal control (actin gene). Class I genes that gain H3K9m2 in *met1* have the same response to *met1* mutation as some transposable elements such as *TA3*, where H3K9m2 is highly dependant on non-CG methylation. Genome-browser views of these loci are shown on the right. Yellow horizontal bars: protein-coding genes; blue horizontal bars: transposable elements; green bars: dispersed repeats (regions with sequence of homology); orange bars: small RNAs clusters (MPSS); purple bars: tandem repeats **B.** Fraction of H3K9m2 hypermethylated genes in *met1* that contain a transposable element (TE). **C.** Representative views of small RNA accumulation at Class I genes in wild type and *met1* (Arabidopsis Epigenome Browser, AnnoJ, http://neomorph.salk.edu/epigenome/epigenome.html). The 'translucid' reads indicate mapping to multiple locations.

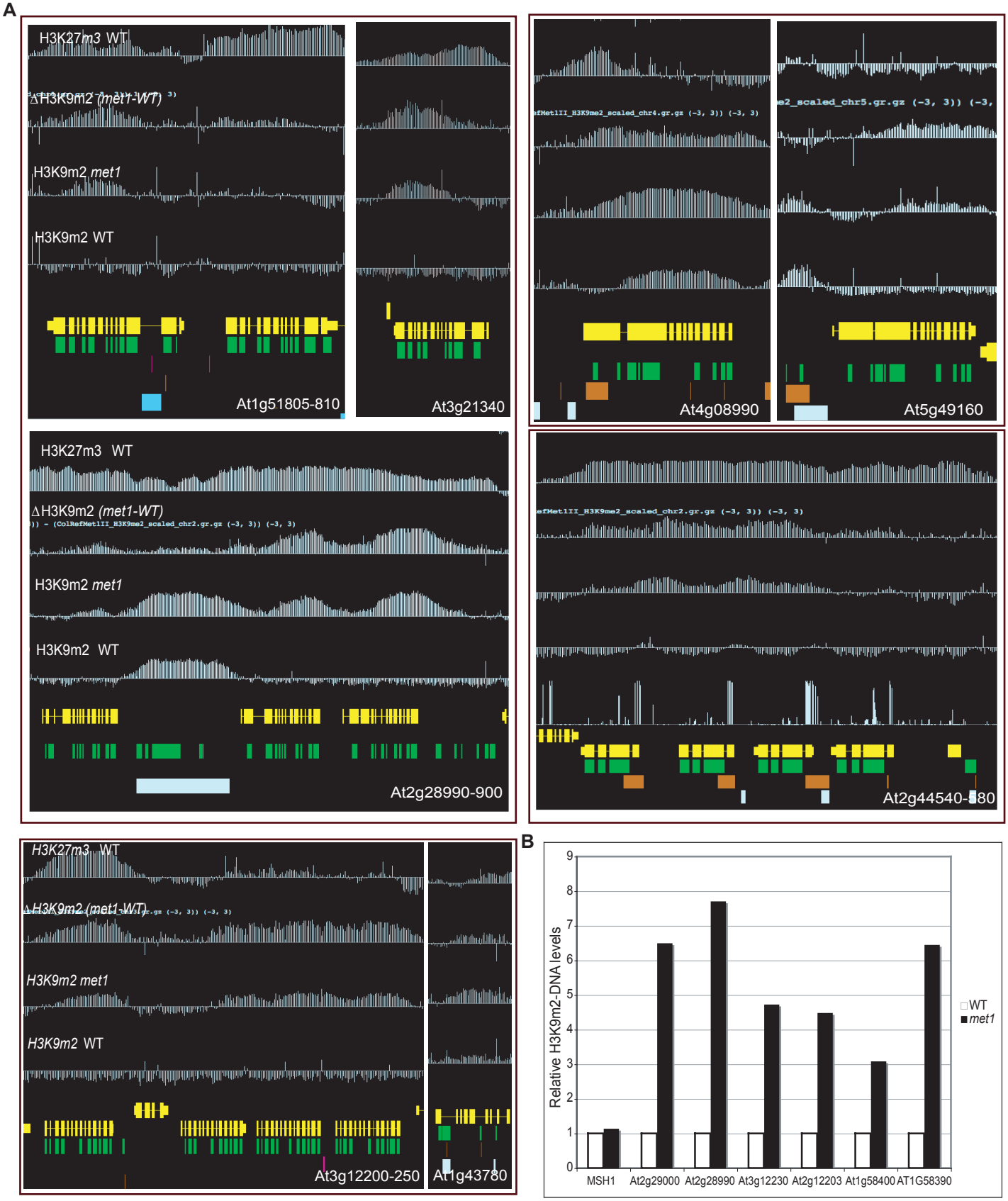

Supplemental Figure 4. Supplementary information on Class II genes. A. Representative genome-browser views of genes (yellow bars) that gain H3K9m2 marks in their coding-region in *met1* and are pre-marked with abundant H3K27m3 in WT. The green bars represent 'dispersed repeats' which show that these genes (in each box) present sequence homology to each other. Left panels: genes homologous to At2g28990 (by their Leucine-rich kinase domains) either linked (AT2g29000, Blast Score to At2g28990 of 5e-29) or unlinked (At1g51805 and At3g21340, Blast Score to At2g28990 of 4e-48 and 3e-67 respectively). AT1g51805 is potential siRNA-generator locus as shown by the presence of tandem repeats (purple bars) and small RNAs (orange bars). Top right panel: At4g08990 is a potential siRNA generator locus for At5g49160. Bottom left panel: SCPL genes; At1g43780 generates siRNAs. Middle right panel: in this example, all the loci shown (glycosyl-hydrolase genes) can produce siRNAs and could potentially target each other in trans in *met1*. **B.** Verification of H3K9m2 state at Class II genes by independent chromatin immunoprecipitation experiments. The immunoprecipitated DNA was quantified by real-time PCR and normalized to the input DNA and to an internal control (Actin gene). For paralogous genes, only primers that hybridize to gene-specific sequences were used.

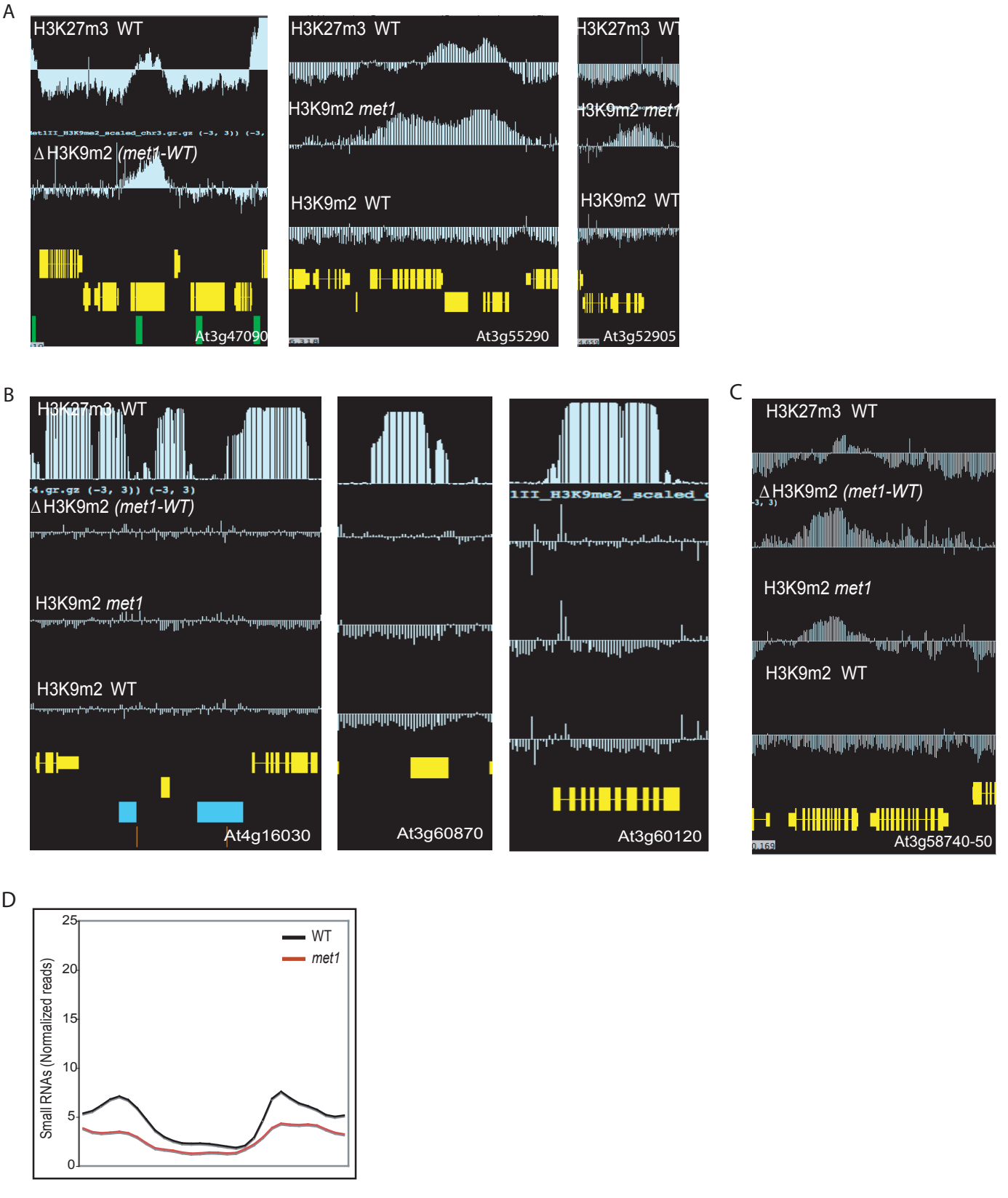

Supplemental Figure 5. Supplementary information on Class II genes. A. Representative views of genes that gain H3K9m2 in *met1* and are H3K27m3-marked in wild-type; however, these genes were not recovered among Class II genes due to their low levels of H3K27m3 in wild-type. This shows that the number of true Class II genes (H3K27m3 in wild type and ectopic H3K9m2 in *met1*) maybe underestimated by our stringencies. Representative IGB view of genes marked with H3K27m3 marks that do not gain ectopic H3K9m2 in *met1*. **B.** Representative views of genes that are marked with H3K27m3 in WT but do not gain ectopic H3K9m2 in *met1*, suggesting that there are additional features that contribute to ectopic H3K9m2 in *met1*. **C.** Representative genome-browser views of two paralogous or related genes that were not retrieved as dispersed repeats by 'Repeat Masker', CITRATE SYNTHASE 1 and 2 genes (At3g58740 and At3g58750). These examples suggest that in the genome-wide analysis shown in Figure 2F, the proportion of genes H3K9m2 hypermethylated in *met1* that correspond to duplicated/paralogous/related genes is underestimated and must be larger than 40%. Yellow horizontal bars in IGB views: protein-coding genes; blue horizontal bars: transposable elements; green bars: dispersed repeats (regions with sequence of homology); orange bars: small RNA clusters (MPSS). **D.** Average distribution of small RNA-seq reads [16] across Class II genes.

A

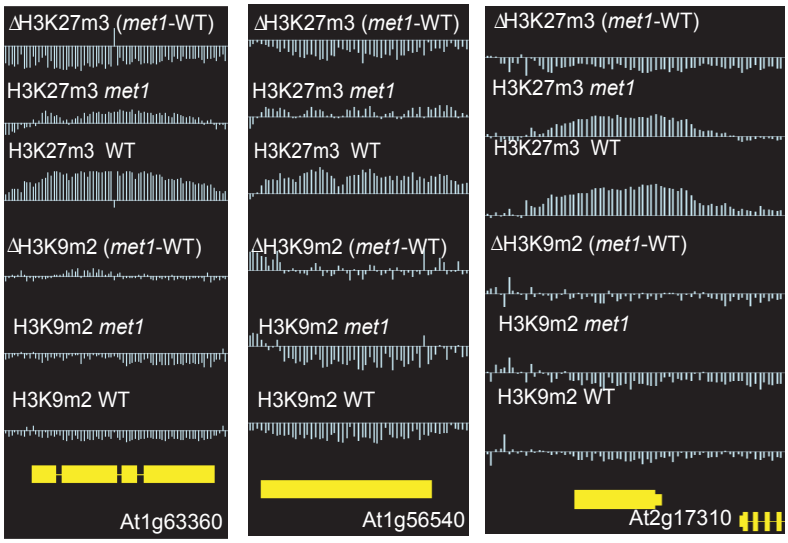

B

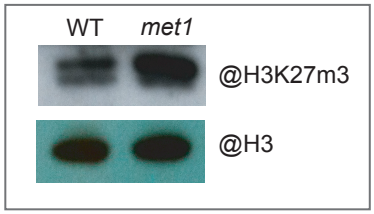

Supplemental Figure 6. Supplementary information on H3K27m3 changes in *met1*. A. Representative views showing PcG-target genes that do not gain H3K9m2 in *met1*, yet lose H3K27m3 marks. **B.** Global accumulation of H3K27m3 marks in WT and *met1* mutants by Western Blot (upper panel). Detection of histone H3 -independently of its modifications- is shown as a loading control (lower panel).

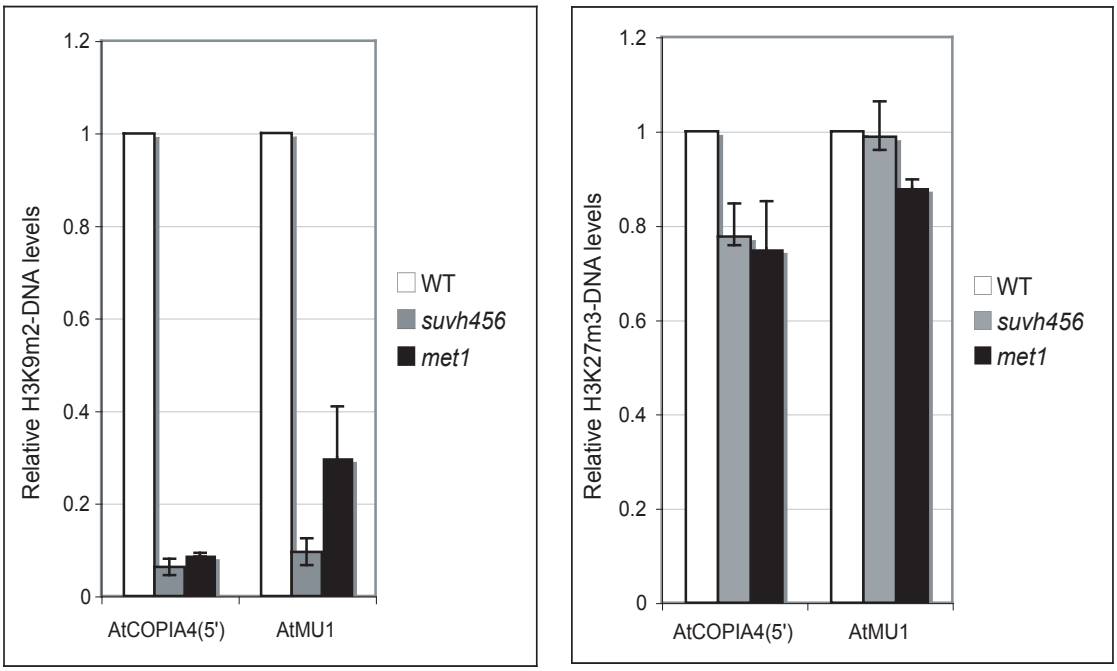

Supplemental Figure 7. Analysis of H3K9m2 and H3K27m3 marks at two transposons by ChIP followed by real-time PCR. Data were normalized to the input DNA and to an internal control (actin gene).

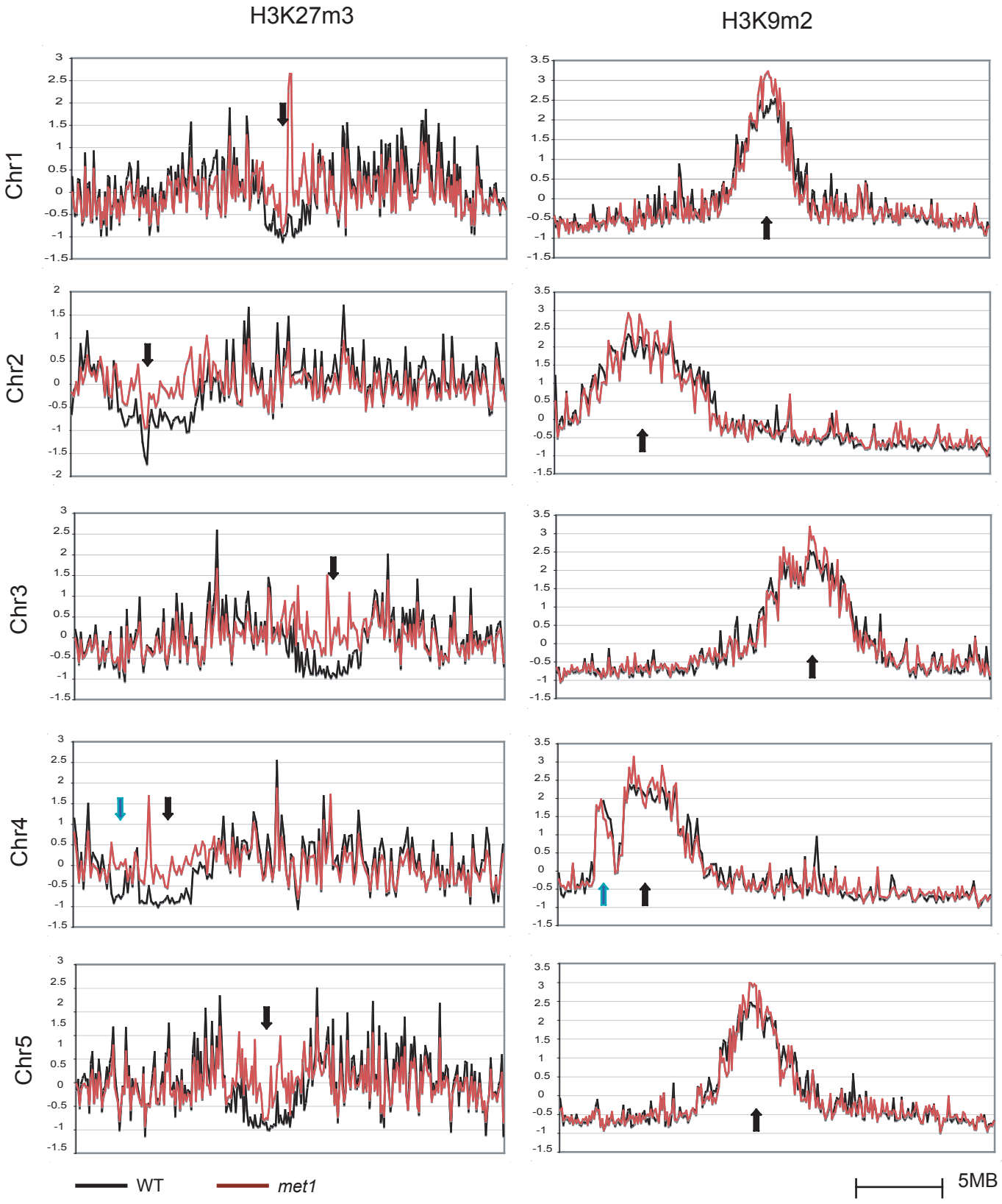

Supplemental Figure 8. Chromosomal distributions of H3K27m3 (left) and H3K9m2 (right). Left and right panels show the normalized levels of H3K27m3 and H3K9m2 respectively in a sliding 100 kilobase windows. The black arrow indicates the centromeric region. The blue arrow indicates the heterochromatic knob on chromosome 4.

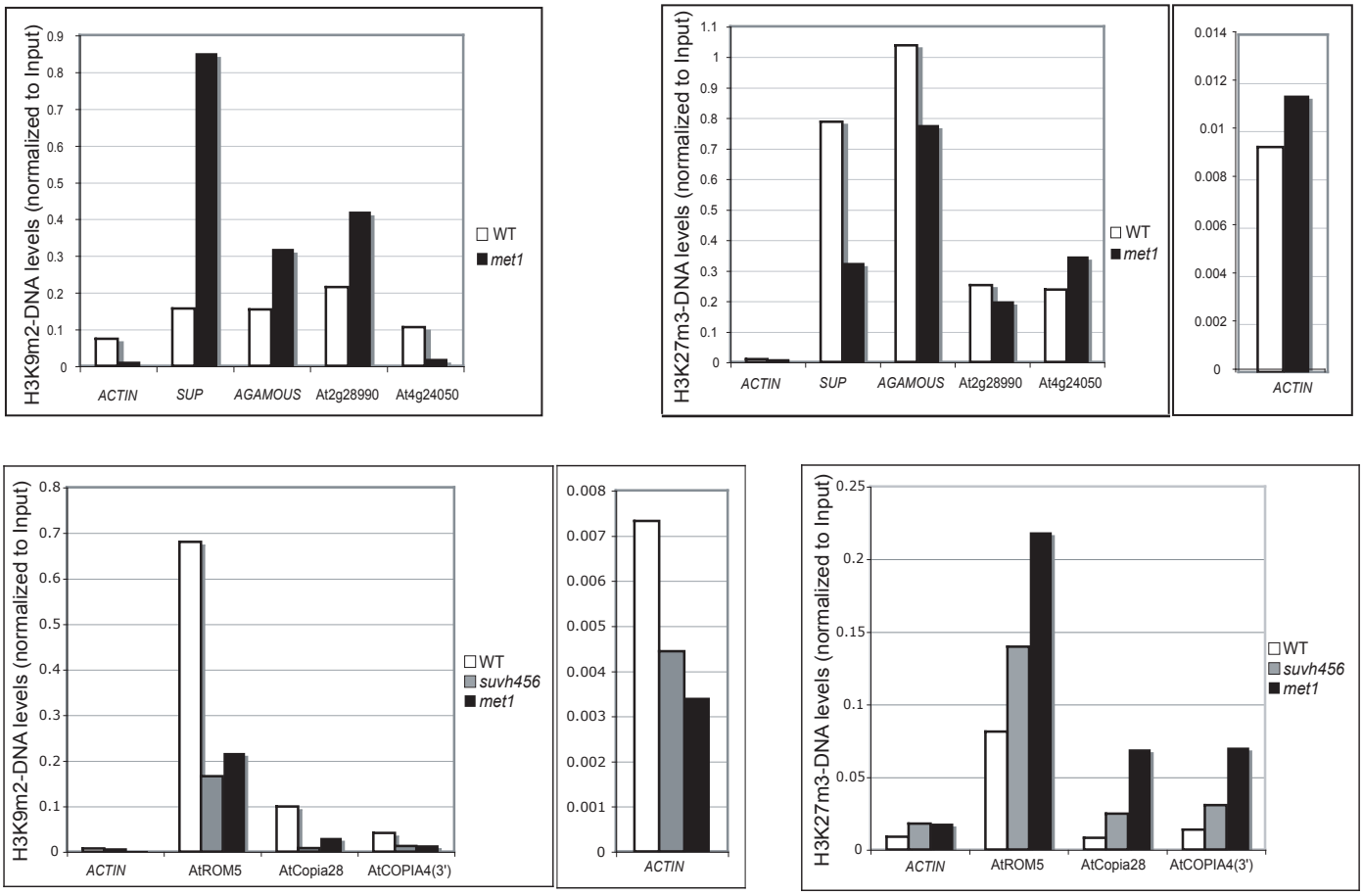

Supplemental Figure 9. Supplementary information on ChIP-chip validation by ChIP-qPCR. Data shown in Figures 4C (top panel) and 5C (bottom panel) are normalized to input, with actin shown as a separate control so that ChIP efficiencies can be visualized. One of the two experiments averaged in Figure 3C and 4C is shown here as a representative graph.